Alumina Hydrate Suspension in the Draft Tube Precipitator Design – Batch versus Continuous Operation

Kumaresan T.[1], Kiran Bhor[2], Vilas Tathavadkar[3], Ashish Mishra[4], Prasanta Bose[5] and Rohit Chourasia[6]
1. Senior Scientist (Metals and Mining)
2. Senior Scientist (Metals and Mining)
3. Senior Vice President & Function Head (Metals and Mining)
Aditya Birla Science and Technology Company (P) Ltd., Navi Mumbai, India
4. Assistant Manager (Production)
5. General Manager (Technical)
6. Head (Production)
Hindalco Industries Limited, Muri, India
Corresponding author: kumaresan.t@adityabirla.com

Abstract

Industry scale draft tube precipitator designs for the Bayer process have the task to uniformly suspend alumina hydrate particles with minimum power consumption. During operation, the hydrate concentration in the overflow will be uniform if particles are uniformly suspended in the entire precipitator volume, otherwise gradients in hydrate concentration may prevail. The strength of the draft tube pumping capability and the nature of the annular region flow pattern determines the quality of hydrate suspension in the entire precipitator volume. Batch operation exhibits an axial up flow pattern in the annular region. However, when draft tube precipitators are connected in series through launders, the annular region flow pattern converts to swirling flow that affects hydrate suspension. Consequently it is vital to maintain the characteristic flow pattern required for hydrate suspension during continuous operation.

Keywords: Alumina precipitator, mixing, draft tube, swirl flow, hydrate suspension.

1. Introduction

In the Bayer precipitation area, the overall economics of the process depends on the recovery of alumina by seeded precipitation from the caustic aluminate liquor, and the production of alumina trihydrate with a desirable size distribution. This result depends on favourable conditions of temperature, supersaturation, particle concentration, shape and size. Precipitation processes are of great industrial importance in the chemical, pharmaceutical and metallurgical process industries.

Loh et al. (2000) concluded that the precipitation process is the rate determining step in the production of aluminium hydrate by the Bayer process [1]. This unit process not only determines the productivity but also the product qualities of size and strength. When the local environment is supersaturated, the particles tend to grow, while on the other hand when the local environment is saturated or unsaturated, the particles tend not to grow or to dissolve.

The mixing in large scale vessels can determine whether favourable or non-favourable conditions for precipitation exist. Green (2002) indicated that to a large extent, convective mixing determines the macro-environment both temporally and spatially and the in-homogeneity in the macro flow pattern ultimately affects the local environment of temperature, supersaturation and particle concentration [2].

Bourne and Sharma (1974) studied the effect of draft tubes on the critical propeller speed of a particle suspension using the flat-bottomed stirred vessel [3]. They observed a 26% reduction in the propeller critical speed for a particle suspension in the presence of a draft tube. Fort (1986) studied the effect of a draft tube on the flow pattern produced by pitched blade turbines using a conical shaped draft tube, where the diameter gradually varied from top to bottom [4]. It was observed that the average volumetric flow rate increased by ~100% in the presence of a conical-shaped draft tube.

Later, Tatterson (1982) observed that the use of draft tubes in stirred vessels enhanced the circulation time and avoided the short circulation of the flow produced by a pitched blade turbine [5]. Further, he studied the effect of draft tube diameter on the circulation time, observing that the draft tube with smaller diameter gave a lesser circulation time (19.2 %) than the draft tube with larger diameter. The draft tube length was maintained constant throughout the experiments.

The comprehensive study published by Kumaresan et al. (2005) investigated the flow pattern for the narrow draft tube and illustrated the effect of two alternative lengths of a draft tube on the flow pattern and, hence, on the mixing performance [6]. The taller draft tube configuration results in an increase in secondary flow number, and consequent decrease in mixing time by 22%.

Lane (2006) studied the effect of two aspect ratios of draft tube agitation configurations on the flow pattern and particle density distribution [7]. The impeller was modeled as a constant source model in their CFD studies for both the aspect ratio designs. They concluded that the unstable re-circulating vortex bursts transport the particles to the tank surface for the smaller aspect ratio design.

Wu et al. (2012) studied the off-bottom particle settling height for swirl flow rotor configuration, draft tube agitator and multi staged agitator [8]. They justified that the draft tube agitation system is more efficient for particle suspension. Brown et al. (2014) investigated the effect of mesh density with various combinations of turbulence models in the taller aspect ratio tanks using CFD [9]. A simulation with a medium level of mesh density using a momentum source model was compared with the impeller rotation model. The predicted CFD simulation results were validated using laser Doppler anemometer experiments for normalized mean axial velocities.

Previous publications have extensively studied the effect of draft tubes on the flow pattern, circulation time and mixing time in batch stirred tanks. Very few references are available concerning draft tube agitation with a focus on alumina precipitators with taller aspect ratio ($H/T \geq 2$). The present work illustrates the importance of the change in the characteristic flow pattern of draft tube precipitator from batch to continuous operation and its impact on the hydrate suspension.

2. Draft Tube Precipitator Design

The brief overview of literature reported above reveals that published investigations put more emphasis on the shorter draft tubes when focused on batch operation. The draft tube precipitator design considered in this study has a tank diameter of 14m, draft tube diameter of 4.6m, liquid height of 36m and draft tube height of 27m. The higher aspect ratio design ($H/T > 2$) in refineries always helps to minimize the energy consumption compared to air lift agitation or multistage mechanical agitators.

The Lightnin C110 down pumping impeller located inside the draft tube occupies around 90 % of the area of the draft tube. The draft tube is fitted with flow straightening vanes, located just below the impeller. These vanes guide the slurry downwards inside the draft tube with minimum swirling (Landberg. 1970) [10]. The draft tube has six columns of slots extending from the bottom to 50 % of the draft tube height. Slots are mandatory to afford slurry communication to equalize the pressure inside and outside the draft tube. It is important to understand that the slots not only provide for slurry/liquor flow during particle settling, but they play a major role in equipment stability during normal operation [10]. In view of this, it was decided to undertake a systematic study using computational fluid dynamics (CFD) to investigate the flow pattern and particle suspension behavior in the draft tube agitation. A sketch of the geometry corresponding to the commercial scale conditions studied is given in Figure 1.

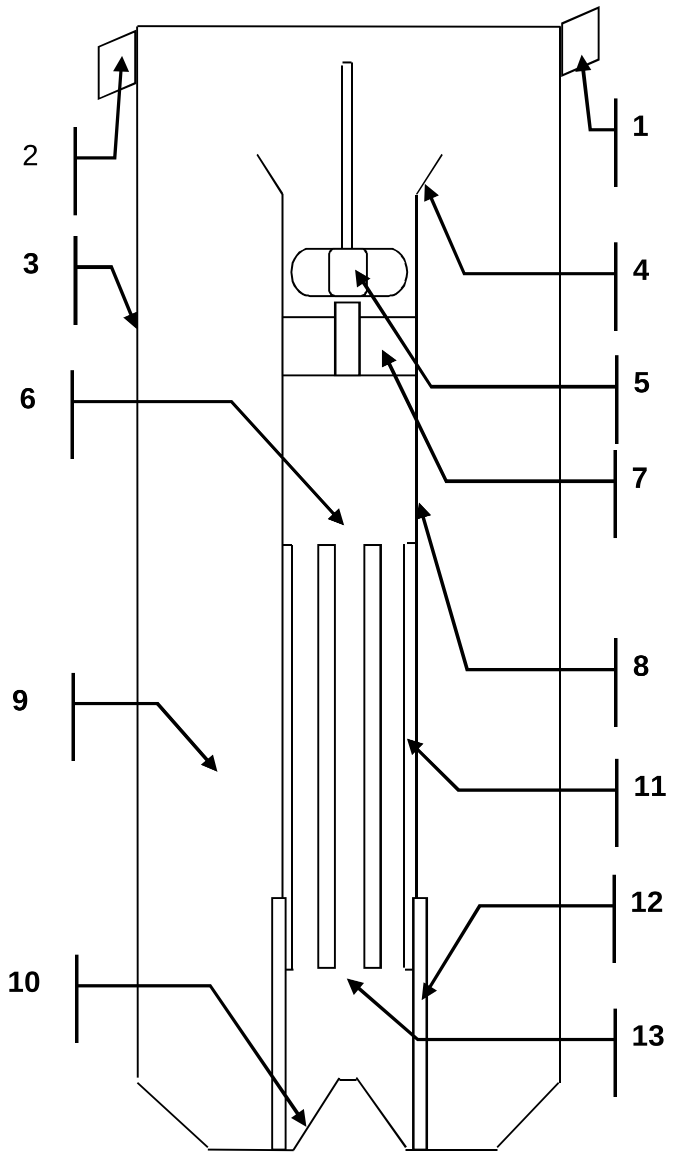

Figure 1. Draft tube Details.

Numbered elements from Figure 1 above: (1) Inlet (2) Outlet (3) Precipitator wall (4) Draft tube bell-mouth suction (5) Hydrofoil impeller (6) Draft tube region (7) Flow straightening vanes (8) Draft tube wall (9) Annular region (10) Profiled precipitator bottom (11) Draft tube slots (12) Draft tube support (13) Draft tube outlet.

3. Modeling and Simulation

3.1. Impeller Modeling

In general, for economic reasons, commercial scale draft tube precipitators typically vary from 10 to 12m in diameter and up to 40m in height [7]. It is very important to note that the effect of rotating impeller produces an overall swirl flow pattern. In 3D ultrasonic jet flows, a small initiation of the tangential component (which may arise out of non-vertical or marginal off-center horn position) will finally impart a greater deviation on the axial/radial direction velocities and hence the broadening of jet occurs in the axial direction (Kumar et al. 2006, Kumaresan et al., 2006) [11, 12]. However, the proportion of the strength of the individual components of velocities may vary between process equipment that produce jet flows.

Harvey et al., (1996) and Weetman (1997) found that the moving reference frame predicted the mean velocities well especially near the impeller boundary [13,14]. The overall model predictions were within 20% throughout the vessel [13]. Most of the previous works have successfully predicted the mean flow pattern both qualitatively and quantitatively for the bulk flow away from the impeller for the standard impeller-vessel configurations using shorter aspect ratio tanks. In the present study, the CFD simulations were carried out using Lightnin C110 type impeller rotating at 38 rpm and the impeller rotation is modeled by the moving reference frame (MRF) technique.

3.2. Turbulence and Particle Modeling

Aeschbach and Bourne (1972) optimized the continuous flow crystallizer design with respect to the tank and draft tube geometry through experiments [15]. Hoekstra et al., (1999) used the k- ε turbulent model and a Reynolds stress transport equation model for a strong confined swirling flow [16]. The results predicted by k- ε model showed a large discrepancy between the measured and predicted velocity fields.

Brown et al. (2014) compared CFD simulated results with laser Doppler anemometer experimental mean/RMS velocities and concluded that the RSM model is able to predict the key features of the flow in the taller aspect ratio precipitation tank [9]. Also, it is known that the RSM model helps predict the complex flow streamline curvature, swirl, rotation and high strain rates flow. In the present work, 90% of the draft tube cross sectional area is covered by the impeller rotation at the impeller location. The close proximity of impeller rotation and fluid interaction with draft tube wall will cause high intensity strain rates due to swirl flow generation and breakage. Consequently, it was decided to carry out the simulations using the standard RSM turbulence model.

The governing conservation equations of fluid flow represent mathematical statements of the conservation laws of mass (continuity) and momentum. Turbulence for the fluid phase was modeled using a standard RSM turbulence model. The Reynolds stress model (RSM) makes use of transport equations for all six independent components of the Reynolds stress tensor and an equation for the energy dissipation rate.

The equation of turbulent stresses contains the terms; pressure rate of strain (which contains fluctuating pressure and velocity gradients) and the flux of Reynolds stresses. In addition to the modeling of the terms in the turbulent energy dissipation rate equation, these terms need to be modeled. Therefore, though RSM takes into consideration the transport of turbulent stresses, its parameters are not universal (i.e., the model should be calibrated for different types of flows).

Continuity equation $$\nabla \bullet (\rho U) = 0 \quad (1)$$

Momentum equation $$\frac{DR_{ij}}{Dt} = P_{ij} + D_{ij} - \varepsilon_{ij} + \prod_{ij} + \Omega_{ij} \quad (2)$$

where R_{ij} is the transport term by convection,

P_{ij} is the rate of production,

D_{ij} is the transport by diffusion,

ε_{ij} is the rate of diffusion,

$\prod_{ij}$ is the transport due to the turbulent pressure-strain interactions and

Ω_{ij} is the transport due to rotation.

The approach in RSM is to solve for Reynolds stresses from individual transport equations for each Reynolds stress. The Reynolds stress equation consists of convection, production by the effects of mean strain term, diffusion, pressure-strain and dissipation terms. The production term is the transfer of energy from the mean flow to the turbulence. This term is calculated from mean flows and Reynolds stresses where they do not need modeling. The diffusion consists of three components: the turbulent diffusion involving triple products, the viscous diffusion involving molecular viscosity and pressure diffusion involving mean pressure. The viscous diffusion is exact and does not need modeling. Only turbulent and pressure diffusion terms need to be modeled accurately.

3.3. Particle Suspension

In the annular region of the draft tube agitator, the fluid flows in the upward direction along with the swarm of dense particles. The downward pull of gravity and the upward pull of the drag force of the upward-flowing fluid act on the particles. If the fluid velocity is increased, the pressure drop increases until it equals the weight of the dense particle swarm bed on the cross-sectional area. This velocity is called the minimum fluidizing velocity. When this point is reached, the particle density will expand uniformly. As soon as the velocity increases beyond the minimum fluidization velocity, the particles tend to flow in the upward direction. It is important to assure that the velocities in the entire annular region are very much greater than minimum fluidizing velocity, so that particles tend to be in suspended flow.

The hydrate particle flow was simulated using the Eulerian-Lagrangian one way coupling approach, implying that momentum is transferred from the liquor to the hydrate particle, so that the hydrate particle is transported but this does not affect the fluid. Consider hydrate particles travelling in a continuous fluid medium. The forces acting on the particle which affect the particle acceleration are due to the difference in velocity between the particle and fluid, as well as to the displacement of the fluid by the particle. In the Particle transport modeling, the hydrate particles are tracked through the flow in a Lagrangian way.

The total flow of the hydrate phase is modeled by tracking a small number of particles through the continuous fluid. Individual particles are tracked from their injection point until they completely distribute inside the domain. Each particle is injected in turn, to obtain an average of all particle tracks and to generate source terms for the fluid mass and momentum equations. The fluid affects the particle motion through the viscous drag and a difference in velocity between the particle and fluid. Conversely, there is a counteracting influence of the particle on the fluid flow due to the viscous drag. This effect is termed coupling between the phases. In the present study, the interaction between the fluid-particle phases is coupled one way i.e., the fluid is allowed to influence trajectories but particles do not affect the fluid.

The tracking is carried out by forming a set of ordinary differential equations in time for each particle, consisting of equations for the position and velocity of species. These equations are then integrated using a simple integration method to calculate the behavior of the particles as they traverse the flow domain as mentioned in ANSYS-CFX 14. In the work of Lane [7], four hydrate particle sizes have been tested (20, 55, 85 and 145 microns).

Also, in the work of Wu et al. [8], they experimented using a larger height to diameter ratio (H/T=2), and considered particle size of d75 = 120 micron for their cold flow lab experiments. Considering the aspect ratios and particles sizes, in the present work the hydrate particles are assumed to be spherical and the settling studies are done for the particle size distribution which has a Rosin Rammler mean size of 130 micron, with the power of 2.5 factors for both for the batch and continuous tanks. The drag model used in the present work is the Schiller Naumann drag Model.

$$C_D = \left(\frac{24}{N_{\text{Re}}} (1 + 0.15 N_{\text{Re}}^{0.687}) \right) \tag{3}$$

Where C_D is the Drag coefficient (-) and N_{Re} is the Reynolds number (-).

Once the single phase flow pattern is established, the hydrate particles are injected near the draft tube inlet and the particle equation is solved in the one way coupling framework. The numerical domain is meshed using ANSYS-ICEM which has 46, 82, 000 tetrahedral elements and the simulations are carried out using ANSYS-CFX 14.

4. Results and Discussions

4.1 Annular Region Flow Pattern

Figures 2A and 2B shows the comparison between the axial velocity vector flow pattern of batch design and continuous flow design. The impeller rotates in the clockwise direction at the rate of 38 rpm and this generates a tangential flow, and inducing a swirl flow effect which is very clearly visible from the top of the tank. This is very much evident in both batch and continuous flow design as seen from the Figures 2A and 2B in the conical mouth of the draft tube. It is also clear that the upward velocity vector pattern in the annular region of the tank is differing from batch to continuous design.

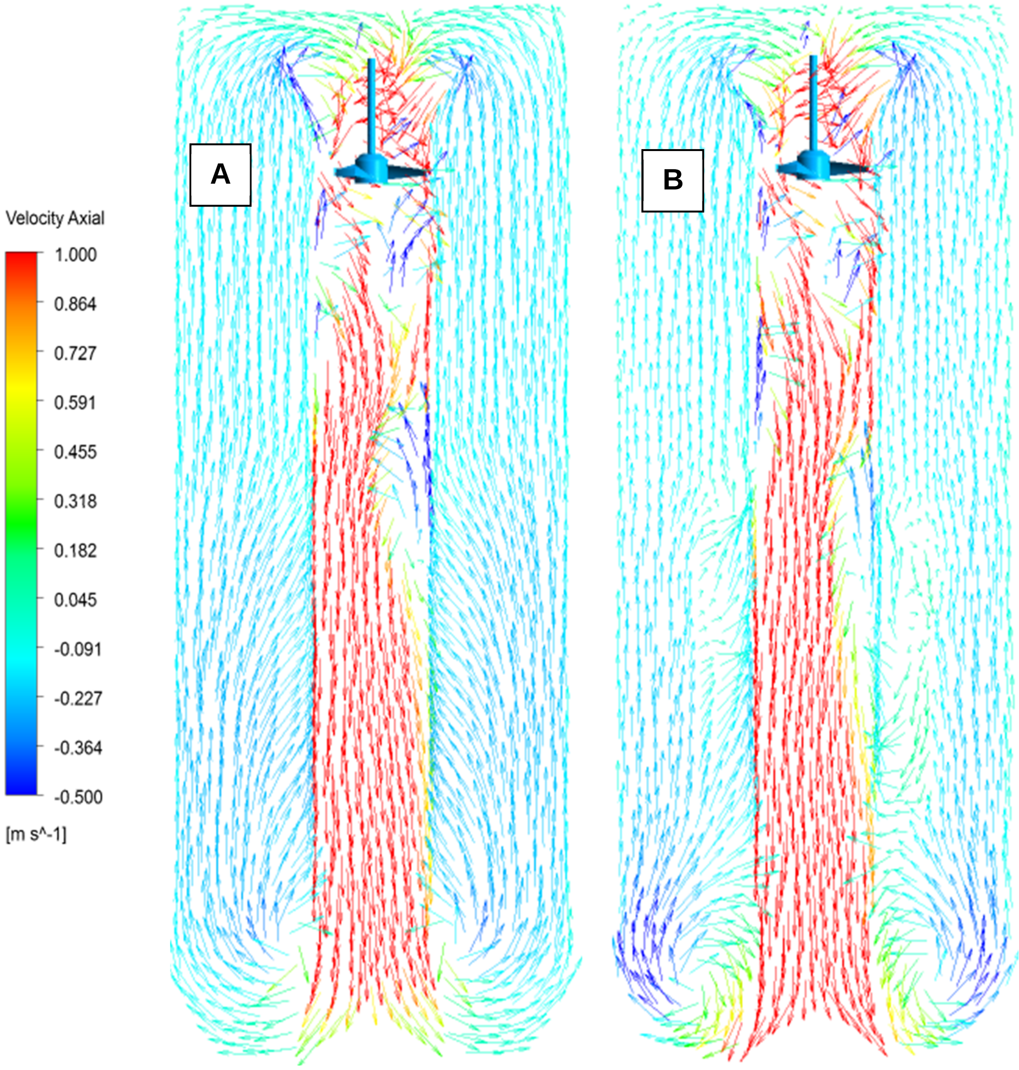

Figure 2. Axial velocity vectors in the precipitator (A) Batch design. (B) Continuous design.

The moment downflow reaches the draft tube outlet, the axial pumping flow rate for the batch and continuous design is found to be around 18.77 and 20.60 m^3/s respectively. Due to the existence of a low pressure region inside the draft tube, the slots will have both inflow and outflow through draft tube. Figure 3 shows the flow streamlines in the annular region of the three different precipitator designs. The batch design has uniform upward flow streamlines in the annular region (Figure 3A). But the continuous flow design has a swirl upward flow in the annular region. This swirl nature is induced because of the inlet and outlet launder flow (Figure 3B).

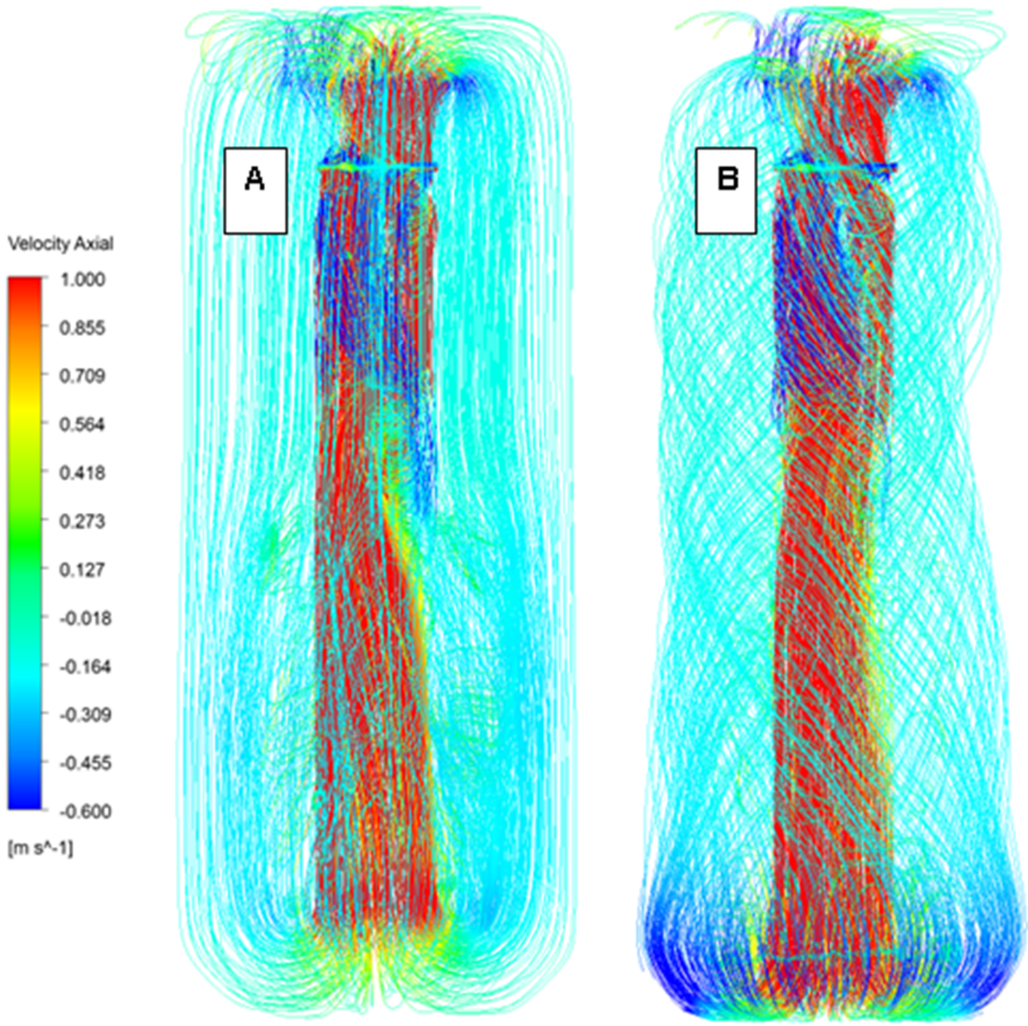

Figure 3. Axial flow streamlines in the precipitator.
(A) Batch design. (B) Continuous design.

4.2 Draft Tube Flow Pattern and Slot Interactions

Figure 4 shows the quantitative flow interaction between the draft tube region and annular region of the batch precipitator model through slots. The batch model does show some fluctuations in flow uniformity inside the draft tube and the downflow inside the draft tube will not be as uniform as constant source model with respect to cross sectional area of the draft tube. The moment the momentum reaches the top portion of the slots (0 - 20% slot height (SH)) from the impeller, there is a considerable suction from the annular region to the draft tube region (Figure 4A).

About + 1.03 m3/s of induced flow rate is observed in the top portion of the slots (0 – 20 % SH). Similarly, + 0.734 m3/s of induced flow rate is observed in the 21 – 40 % of SH portion of the slots (Figure 6A). Nil draft tube suction is found in the remaining portion of the slots (SH < 20 %). However, - 0.58, - 0.90 and - 0.115 m3/s of out flow is evident for SH (21 – 40 %), SH (41 – 95 %) and SH (96 – 100 %) respectively from the draft tube region to the annular region of the batch model (Figure 4B). Generally, slots play an important role during start-up after shutdown of the tank to allow erosion of the settled solids through slots (Lane. 2006; Howk and

Giralico. 2008) [7,17]. It is important to understand that the slots really afford a flow communication to equalize the pressure inside and outside the draft tube to prevent its collapse from inward forces [10].

The impeller rotation creates the low pressure zone inside the draft tube and this region is stretched vertically above and below the impeller zone. This creates more inflow in the batch model than that of the constant source model. The batch model allows to have + 1.77 m3/s of inflow (Figure 4A) and - 1.59 m3/s of out flow (Figure 4B) and the overall draft tube pumping capability at the bottom of the tank slightly increases to 18.77 m3/s.

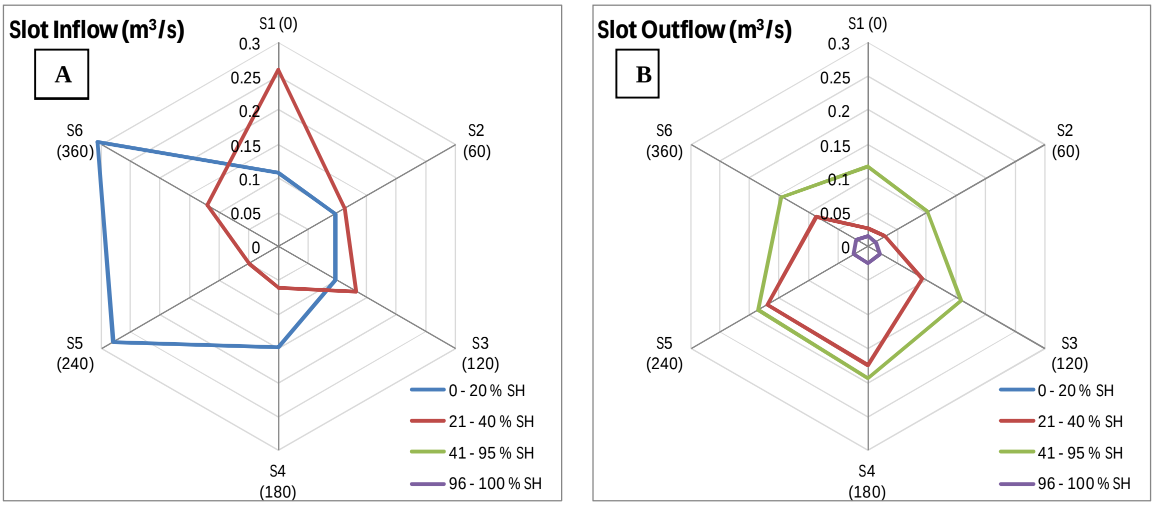

Figure 4. Slot flow interactions in the batch precipitator design.

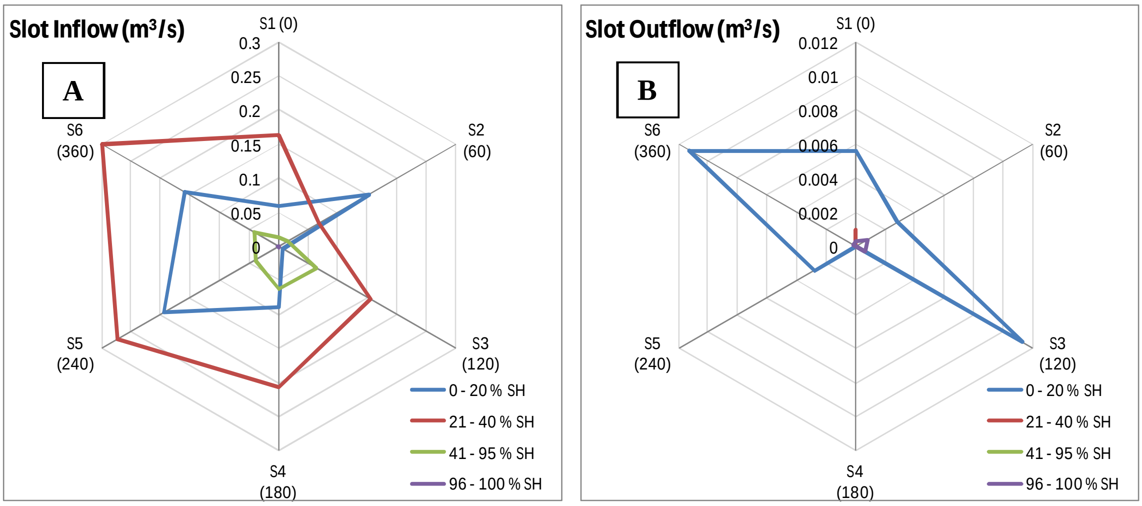

Figure 5. Slot flow interactions in the continuous precipitator design.

Figure 5 shows the quantitative flow interaction between the draft tube region and annular region of the continuous precipitator model through slots. Almost, + 0.66, + 1.16, + 0.238 and + 0.002 m3/s of inflow is evident for SH (0 – 20 %), SH (21 – 40 %), SH (41 – 95 %) and SH (96 – 100 %) respectively from the annular region to the draft tube region of the continuous model (Figure 5A).

Nil draft tube out flow is found in the slot height portion, 41 – 95 % SH. About - 0.034, - 0.001 and - 0.002 m3/s of out flow is evident for SH (0 – 20 %), SH (21 – 40 %) and SH (96 – 100 %)

respectively from the draft tube region to the annular region of the batch model (Figure 5B). The continuous model creates more inflow than that of the batch model. The continuous model allows to have + 2.06 m3/s of inflow (Figure 5A) and - 0.037 m3/s of out flow (Figure 5B), and the overall draft tube pumping capability at the bottom of the tank increases to 20.62 m3/s. In the continuous model, a distinct swirl flow pattern in generated in the annular region of the tank due to the presence of inlet and outlet launder (Figure 3B). The tangential swirl pushes the flow from the periphery of the annular region towards the core region of the precipitator tank. This swirl in the continuous model could probably be responsible for an increase in the overall inflow by 25 % compared to the batch model.

4.3 Particle Suspension

Solid-liquid mixing and suspension is an expensive operation in process industries. The qualitative and quantitative character of the flow pattern especially in the bottom of the mixing tanks is very important to assess the level of suspension or settling for the particular solid-liquid operation.

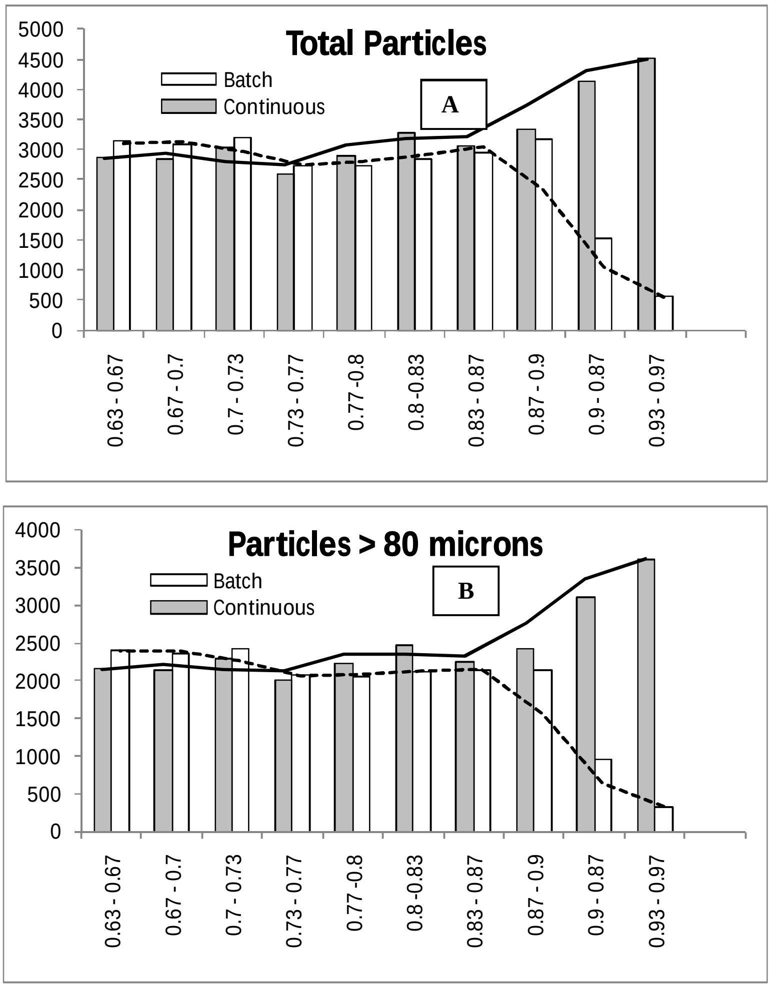

Figure 6. Solid settling in the batch vs. continuous precipitator design.

Figures 6A and 6B show the number of particles both in the batch and continuous tank from the bottom of the tank to 63% of the height of the tank. It is evident that more particles are observed for the height greater than 83% towards the bottom of the tank for the continuous setup. However, in the case of the batch setup, the number of particles greater than 83% height is found to be less than that of the continuous setup. The work of Ayranci et al. (2012), concluded that complete off bottom suspension is critical close to the bottom of the tank, and that solid suspension is dependent upon the combination of mean flow and turbulent eddies, and emphasized that complete off-bottom suspension cannot be achieved without both mean and turbulent flow patterns, and that the balance between the mean flow and turbulent flow is equally important for solid suspension [18]. As inferred from velocity vectors and velocity streamlines, the batch design exhibits a non-swirl flow pattern at the bottom of the tank whereas the continuous design exhibits a swirl flow pattern in the annular region.

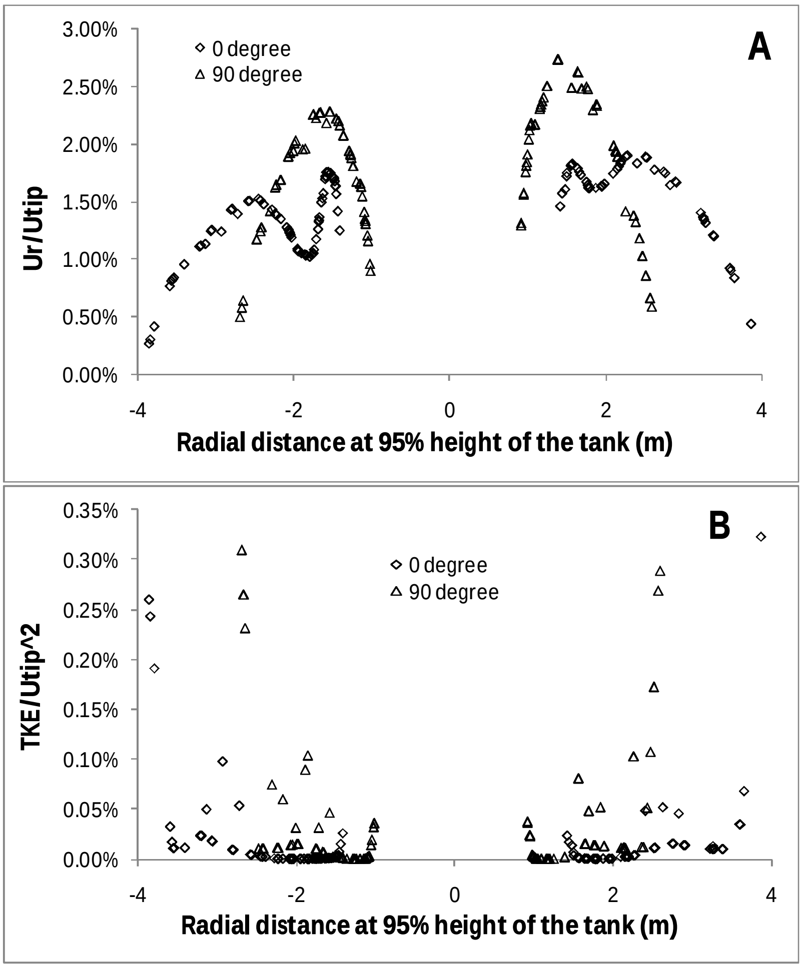

Figure 7. Mean and turbulence near the bottom surface of the batch precipitator design. (A) Dimensionless mean radial velocity. (B) Dimensionless turbulent kinetic energy.

Figure 7 shows the dimensionless radial velocity profiles near the tank bottom that is at the 95% tank height for the batch case. It shows the magnitude of radial velocity is about 1 to 3% maximum of the impeller tip speed near the tank bottom (Figure 7A). Also, the dimensionless turbulent kinetic profiles near the tank bottom at the same location is about 0.3% maximum to that of the square of the impeller tip speed (Figure 7B). Similarly, Figure 8 shows the dimensionless radial velocity profiles near the tank bottom that is at 95% tank height for the continuous case. It shows the magnitude of radial velocity is about 5 to 15 % maximum of the impeller tip speed near the tank bottom (Fig 8A). Also, the dimensionless turbulent kinetic profiles near the tank bottom at the same location are only 0.012% maximum to that of the square of the impeller tip speed (Fig 8B).

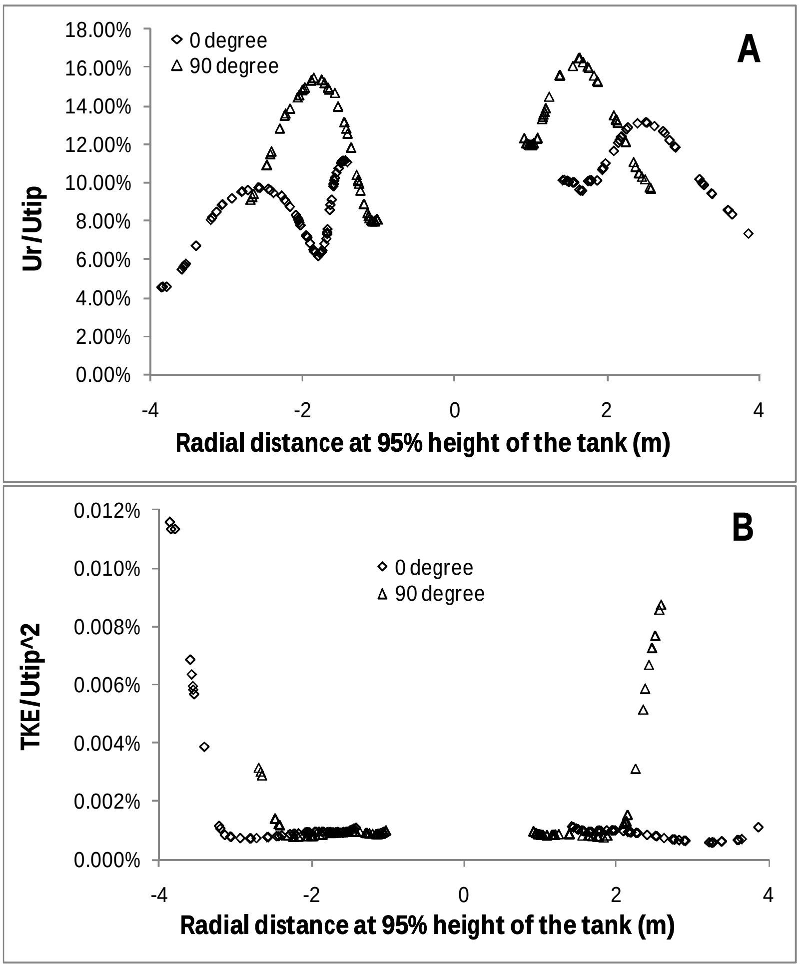

Figure 12. Mean and turbulence near the bottom of the continuous precipitator design. (A) Dimensionless mean radial velocity. (B) Dimensionless turbulent kinetic energy.

This clearly shows that the batch design exhibits a higher level of turbulent kinetic energy at the bottom of the tank than the continuous design. In the work of Ayranci et al. [18], the aspect ratio of the stirred tank is 1 whereas in the present work the aspect ratio is greater than 2 and is a draft tube agitated tank [18]. Due to slot interactions and distance between the tank bottom and impeller source, the final momentum reaching the bottom of the tank will be several magnitudes less than that of the smaller aspect ratio tanks. It can be concluded that solid suspension at the tank bottom needs only 3% maximum of radial mean velocity to that of impeller tip speed and more turbulent kinetic energy for the larger aspect ratio tanks.

5. Conclusions

The batch design predicts a *non-swirl* upflow overall pattern in the annular region of the tank, whereas the continuous design predicts a *swirl* upflow pattern in the same region. The draft tube slots play an important role in the total pumping capability of the draft tube at the tank bottom. The non-swirl flow pattern observed in the batch design produces more homogeneous flow in the draft tube and annular region. The optimum draft tube pumping rate is sufficient for the solid suspension in the taller aspect ratio tanks. It is important to have an optimum type of flow pattern (mean velocity and turbulent kinetic energy) in the tank bottom to reduce settling in alumina precipitators. The industry scale continuous draft tube precipitators must be designed in such a way that the flow in the annular region is non-swirl upward flow.

6. References

1. Loh, J. S. C., Fogg, A. M., Watling, H. R., Parkinson, G. M., Hare, D.O., 2000. A kinetic investigation of gibbsite precipitation using in situ time resolved energy dispersive X-ray diffraction. *Phys. Chem. Chem. Phys*. 2, 3597 – 3604.
2. Green
3. Bourne, J. R., Sharma, R. N., 1974. Suspension Characteristics of Solid Particles in Propeller-Agitated Tanks. 1st European conference on mixing. B3, 25-38.
4. Fort, I., 1986. Flow and Turbulence in Vessels with Axial Impellers. In Mixing: Theory and Practice; Uhl, V. W., Gray, J. B., Eds. 3, 133-195.
5. Tatterson, G. B., 1982. The Effect of Draft Tubes on Circulation and Mixing Times. Chem. Eng. Commun. 19, 141-147.
6. Kumaresan, T., Nere, N. K., Joshi, J. B., 2005. Effect of Internals on the Flow Pattern and Mixing in Stirred Tanks. *Ind. Eng. Chem.* Res. 44, 9951-9961.
7. Lane, G., 2006. Flow instability in an alumina precipitator fitted with a draft tube circulator. 5th Int. Conf. on CFD in the Process Industries, CSIRO, Melbourne, Australia. 1 – 6.
8. Wu, J., Lane, G., Livik, I., Nguyen, B., Graham, L., Stegink, D., Davis, T., 2012. Swirl flow agitation for scale suppression. *Int. J. Min. Proc.* 44, 19-29.
9. Brown, G.J., Whyte, D.S., Fletcher, D. F. 2013. Dynamic flow modelling in precipitator vessels – A study of turbulence modeling approaches. *Applied mathematical modeling.* In press.
10. Landberg, G. G., 1970. Draft tube arrangement for starting-up and settled solids. U.S. patent (3532327).
11. Kumar, A., Kumaresan, T., Pandit, A. B., Joshi, J. B., 2006. Characterization of flow phenomena induced by ultrasonic horn. *Chem. Eng. Sci.* 61, 7410-7420.
12. Kumaresan, T., Kumar, A., Pandit, A. B., Joshi, J. B., 2007. Modeling Flow Pattern Induced by Ultrasound: The Influence of Modeling Approach and Turbulence Models. *Ind. Eng. Chem. Res.* 46, 2936-2950
13. Harvey, A.D., Rogers, S. E., 1996. Steady and Unsteady Computation of Impeller-Stirred Reactors. *AIChE Journal*. 42, 2701- 2712.
14. Weetman, R.J., 1997. Automated Sliding Mesh CFD Computations for Fluid foil Impellers. Proc. 9th Eur. Conf. Mix. 11, 195.
15. Aeschbach, S., Bourne, J. R., 1972. The attainment of homogeneous suspension in a continuous stirred tank. *Chem. Eng. J.* 4, 234 - 242.
16. Hoekstra, A. J., Derksen, J. J., Van Den Akker, H. E. A., 1999. An experimental and numerical study of turbulent swirling flow in gas cyclones. *Chem. Eng. Sci.* 54, 2055 – 2065.
17. Howk, R., Giralico, M., 2008. Stat-up method for draft tube mixing. U.S. patent (7331704 B2).
18. Ayranci, I., Machado, M. B., Madej, A. M., Derksen, J. J., Nobes, D. S., Kresta, S. M. 2012. Effect of geometry on the mechanisms for off-bottom solids suspension in a stirred tank. Chem. Eng. Sci. 79, 163–176.